

## Quasielastic $^{40}\text{Ca}(e,e')$ reaction in the transverse channel: Nuclear structure effects

J. P. Adams and B. Castel

*Department of Physics, Queen's University, Kingston, Ontario, Canada K7L 3N6*

(Received 29 June 1994)

We present a microscopic calculation of the transverse response function for the  $^{40}\text{Ca}(e,e')$  reaction in the quasielastic domain. Our results clearly demonstrate the necessity of including RPA correlations if one wants to describe correctly both position and shape of the quasielastic peak. Building upon the RPA results, we then discuss the importance of the 2p-2h background, which confirms itself to be the dominant mechanism responsible for achieving agreement between theory and experiment at the peak and in the higher energy region. Finally, the results are discussed in the context of the latest relativistic calculations and experimental work.

PACS number(s): 21.60.Jz, 25.30.Fj

It has been over twenty years since the first measurements of the cross section for  $(e,e')$  scattering in the region of the quasielastic peak [1] seemed to substantiate the predictive power of nuclear structure calculations employing the Fermi gas model—the agreement between the predicted and measured responses was certainly enticing. The quasielastic scattering process had a simple interpretation. The incoming electrons were of sufficient energy that the scattering mechanism resembled elastic scattering off free nucleons producing a peak in the scattering cross section at roughly the energy given by the free kinematics. But, because the target nucleons were both moving and bound within the nucleus, the peak was broadened and shifted in energy. It appeared that satisfactory accounting of these nuclear structure effects could be achieved by modeling the nucleus as a noninteracting infinite Fermi gas. However, this agreement between the independent particle model and the measured inclusive scattering cross section turned out to be, to a large extent, fortuitous.

The quasielastic scattering mechanism is really a probe of both the charge and current densities that are produced by the nucleons bound within the nucleus. The cross section is thus a combination of the effects due to two separate channels. The longitudinal channel probes the *charge density* distribution and the transverse channel, the distribution of *current densities*. Of course these two channels are not distinguishable in any single measurement (we observe the superposition of both effects) but a technique known as Rosenbluth separation allowed experimentalists, in 1980, to separate the two channels by exploiting their different angular distributions [2]. A marked disagreement was discovered between the experimental results and the theoretical predictions even though the theoretical models could account quite well for the unseparated cross section. What Altemus *et al.* first demonstrated was that the strength in the longitudinal channel was up to 50% lower than predicted whereas the strength in the transverse channel was in good agreement with theoretical predictions with only slight discrepancies in the shape and position of the peak.

A well known sum rule predicts that the integrated cross section in the longitudinal channel should be proportional to the total charge of the nucleus [3]. Thus if the longitudinal cross section is quenched, the reduction in the integrated cross section indicates a lowering of the effective charge of

the nucleus. As more experiments confirmed a quenching of the response in the longitudinal channel for a wide variety of target nuclei [4–8], the discrepancy between theory and experiment became known as the *missing charge problem*. A great deal of attention has been devoted to the physics of the longitudinal channel [9–23] and, while this work did demonstrate that there are a number of physical processes capable of generating some quenching of the longitudinal response, it did at the same time reveal some more subtle difficulties in our understanding of the transverse response. Virtually all mechanisms that were invoked to improve the theoretical situation in the longitudinal channel were found also to produce quenching in the transverse thus creating a discrepancy where none before had existed. If we wish to claim a full understanding of this scattering process it is vital that effects of all physical processes that are determined to affect the longitudinal response also be considered for calculations of the transverse.

One of the most fruitful avenues in attacking the missing charge problem has been to consider the effects of nucleon-nucleon correlations that go beyond the usual random phase approximation (RPA); including nucleon-nucleon correlations up to RPA order generally produces too much strength in the longitudinal channel and underestimates the strength in the transverse. Many investigators have found that accounting for many-particle–many-hole correlations does indeed produce significant quenching in the longitudinal channel. Addressing the transverse response, Alberico *et al.* introduced the effects of 2p-2h correlations into an RPA calculation based upon a Fermi gas description of the nuclear structure and did find significant improvement in the agreement with experiment [24]. They found that in  $^{40}\text{Ca}(e,e')$  scattering at a momentum transfer of  $2.08\text{ fm}^{-1}$ , there was an almost linear increase in the transverse response up to an energy of 200 MeV. In fact, above 160 MeV the 2p-2h effects were found to be the dominant mechanism for producing strength, a result that is at least a little troubling.

The present work has been undertaken to reexamine these conclusions. Our aim was to first complete a calculation of the RPA response using a more realistic description of the ground state wave functions to clarify more exactly the nature of the discrepancy and investigate any possible finite size effects. We then focused on an explicit calculation of the effect of including virtual 2p-2h states in the description of the target nucleus.

Our paper is organized so as to describe first the RPA calculation of the transverse response function,  $R_T$ , using a fully self-consistent Hartree-Fock basis. The results obtained for  $^{40}\text{Ca}$  clearly demonstrate the importance of including RPA correlations if one wants to correctly predict the position and shape of the quasielastic peak. Also, our results find significantly more strength in the dip region than similar calculations performed using a Fermi gas basis [24]. Building upon our RPA results, we then present a calculation of the 2p-2h background, which confirms itself to be the dominant mechanism responsible for achieving agreement between theory and experiment both in the region of the peak and at slightly higher energies. Our calculation also suggests that much of the strength in the higher energy region should be ascribed to higher order correlations together with more exotic mechanisms like  $\Delta$ -hole and meson exchange currents. Finally, we conclude our work with a critical evaluation of our results together with some recommendations for future experimental and theoretical work.

The fundamental quantity in the method applied here is the particle-hole Green's function  $G(\mathbf{r}, \mathbf{r}', \omega)$ . The response function  $R_T$ , defined in Ref. [3], can be calculated in a coordinate space formalism as

$$R_T \equiv \sum_i |\langle f | \hat{\mathbf{O}}_T | i \rangle|^2 \delta(E_f - E_i - \omega) \\ = \frac{1}{\pi} \text{Im} \int d\mathbf{r} \int d\mathbf{r}' \mathbf{O}_T^*(\mathbf{r}) G(\mathbf{r}, \mathbf{r}', \omega) \mathbf{O}_T(\mathbf{r}'), \quad (1)$$

where  $G(\mathbf{r}, \mathbf{r}', \omega)$  is the particle-hole Green's function. Also,  $\mathbf{O}_T$  denotes the transverse scattering operator, which can be written explicitly as

$$\hat{\mathbf{O}}_T = (\boldsymbol{\sigma} \times \mathbf{q}) \tau_3 e^{i\mathbf{q} \cdot \mathbf{r}}, \quad (2)$$

if only the dominant isovector part of the magnetization current is considered.

The calculation of the transverse response was carried out at three different values of momentum transfer  $q$ . This was done in order to cover the range over which most experiments have been carried out. It was necessary to expand the transverse operator in terms of spherical harmonics each carrying a specific angular momentum  $\hbar\lambda$ . The total response comprises the sum of these terms, which we found to converge by including terms up to  $\lambda=15$  with the dominant contributions coming from values of  $\lambda$  between 5 and 7 depending on the momentum transfer.

The bare Green's function  $G^0(\mathbf{r}, \mathbf{r}', \omega)$  used in computing the free response was generated from Hartree-Fock ground state wave functions calculated in a coordinate space formalism using a Skyrme-like parametrization of the nucleon-nucleon interaction (SGII). We should note that this is a totally self-consistent calculation for noncorrelated nucleons. Figure 1 shows the results for the free response calculated using the bare Green's function; we observe qualitatively a broad peak centered in energy at approximately  $q^2/2M$  as we would expect for scattering from individual nucleons. However, in this range of momentum transfer, the effective particle-hole interaction in the transverse channel is well known to be repulsive in character [25] and thus including the effects of correlations tends to quench the response and push it up to higher energy.

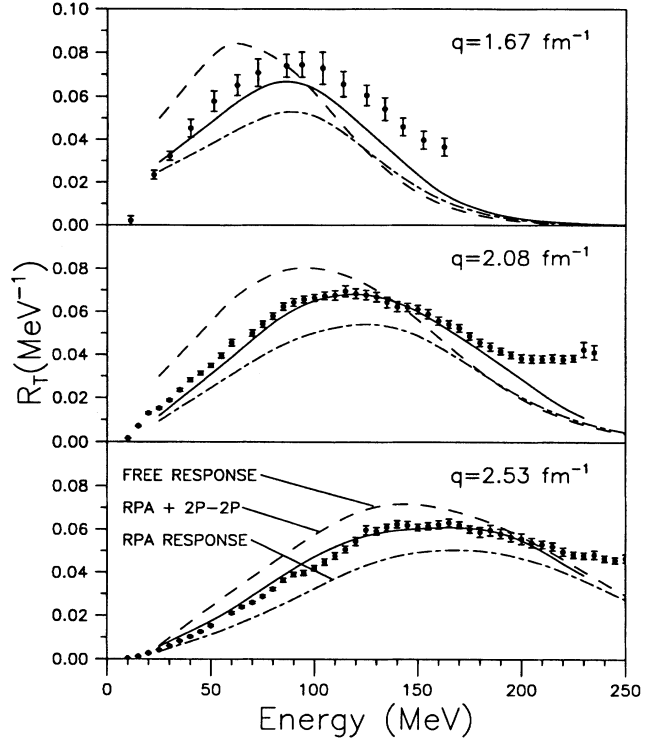


FIG. 1. The transverse response function,  $R_T$ , displayed as a function of energy transfer for three values of momentum transfer. The dashed line denotes the free response, the dot-dashed line includes the effects of RPA correlations, and the solid line includes the effects of 2p-2h correlations. The experimental data at  $q=1.67 \text{ fm}^{-1}$  are taken from Ref. [6] and the data for  $q=2.08 \text{ fm}^{-1}$  and  $q=2.53 \text{ fm}^{-1}$  are taken from Ref. [8].

The effect of RPA correlations was calculated by solving the RPA Green's function equation [26,27],

$$G^{\text{RPA}} = G^0 / [1 + (\delta V / \delta \rho) G^0], \quad (3)$$

within the Hartree-Fock basis. The results, also displayed in Fig. 1, clearly show the expected shift towards higher energy and the overall quenching of the response. As we will see later, the shift in peak position is required for agreement with experiment but the effect of the RPA correlations is to reduce the calculated strength to below the observed value. This is similar to the trend found by Alberico *et al.* This result serves as confirmation of the need to search for models that go beyond the 1p-1h regime in an attempt to fully explain the strength throughout this region. It is worth noticing that our result produces significantly more strength at higher energies than the result calculated in the Fermi gas model. This is comforting because it reduces, to some extent, the need to invoke other mechanisms to explain the missing strength in the dip region.

We now examine the effects of including higher order correlations that are not included in the RPA. The motivation for this is twofold. First, it is a natural extension of any calculation to try to estimate the magnitude of those terms that have been ignored; the 2p-2h correlation terms are the next simplest type of contribution that we can consider if we limit ourselves to nuclear structure effects. Second, many

authors [11,15,18,22] have invoked 2p-2h effects to explain the apparent quenching of the experimental response relative to model predictions in the longitudinal channel; it is natural then to ask what is the effect of the same types of correlations on the transverse response. In our investigations of the longitudinal response [11] we have employed an operator projection technique to account for the effects of many-particle–many-hole correlations. However, because of the more complicated form of the transverse scattering operator, we are unable to exploit this technique for the current problem. We have chosen instead to perform an explicit calculation of the contributions to the transverse response arising specifically from virtual 2p-2h states in the target nucleus.

We started our calculation by determining first the amplitude of virtual 2p-2h states in the ground state of the target nucleus using a harmonic oscillator basis including up to  $10\hbar\omega$  excitations. These amplitudes are of the form

$$a_i = \langle (p'h') J' M' T' M'_T (ph) J M T M_T | V | \hat{0} \rangle, \quad (4)$$

which gives the strength for the excitation of a 2p-2h state comprising two 1p-1h excitations labeled as  $(p'h')$  and  $(ph)$ . These amplitudes were calculated using first order perturbation theory with the residual interaction taken as the pion and rho meson exchange interaction including a contact term [28]. The expression for the matrix elements of this interaction was determined by Oset, Toki, and Weise [29] in their seminal paper on the pionic modes of excitation in nuclei. The exact form is given in the Appendix.

The amplitudes for excitations induced by the transverse operator,  $\hat{\mathbf{O}}_T$ , were then calculated by summing over all possible 2p-2h final states at a fixed excitation energy subject to the constraints imposed by angular momentum conservation. This procedure required performing an angular momentum decomposition of the operator with the component of the operator carrying angular momentum  $\hbar\lambda$  expressed as

$$\hat{\mathbf{O}} = \sum_{\lambda l} i^l f(r) (Y_{ls})^\lambda j_l(qr), \quad (5)$$

where  $s$  is the spin operator ( $s \equiv \sigma/2$ ) and  $f(r)$  is given by

$$f(r) \equiv i4\sqrt{\pi} q \mu \sqrt{2l+1} \langle l01\mu | \lambda \mu \rangle. \quad (6)$$

The isospin operator  $\tau$  has been suppressed in this expression since we are focusing on the angular momentum recoupling. The transverse response function can then be written

$$R_T = \sum_{\lambda\mu} \frac{1}{2\lambda+1} \left| \sum_{ik} a_i \langle (2p2h)_{k\lambda\mu} | \hat{\mathbf{O}}^\lambda | (2p2h)_{i00} \rangle \right|^2. \quad (7)$$

The sum over  $i$  and  $k$  refers to all possible final states  $k$  consistent with each of the virtual states  $i$  appearing with amplitude  $a_i$ . The explicit form of the matrix element between 2p-2h states is given in the Appendix. In the actual calculations, the sum over angular momentum transfer was truncated at  $\lambda=20$ , at which point the series had clearly converged within the required accuracy of the calculation.

Because the final states were treated as bound states our results were necessarily on a discrete energy spectrum and were therefore broadened by folding with a Lorentzian distribution, a procedure to which the final results were quite insensitive.

The results obtained for the 2p-2h strength as a function of excitation energy were then combined with the RPA calculation described earlier to produce a final value for the transverse response function,  $R_T$ . Figure 1 now shows the final results of our calculation at three different values of the momentum transfer. We observe that the agreement with experiment is very good in the region of the quasielastic peak although at the lower momentum transfer value the calculated result still slightly underestimates the observed strength. It is comforting that the results in the region of the peak show such good agreement with experiment since this is the energy range in which our model would be expected to be the most reliable. Beyond the quasielastic peak our calculation begins to underestimate the total strength. This is to be expected since this is the region in which the additional degrees of freedom such as the delta resonance and meson exchange currents become important. Also, there is no reason to limit ourselves to 2p-2h excitations and thus contributions from 3p-3h, 4p-4h, etc., might also be expected to contribute at higher energy.

Two major differences now emerge from a comparison of our results with those of Alberico *et al.* using the Fermi gas model. First, the results using the Fermi gas model tend to overestimate the strength in the low energy part of the spectrum where our results are in better agreement. Second, our 2p-2h results show convergence at higher energies and always contribute a relatively small background relative to the dominant 1p-1h response. The 2p-2h “background” of Alberico *et al.*, in contrast, appears to be unbounded at higher energies and, in fact, becomes dominant over the RPA results above 160 MeV. This, in our opinion, leads to some theoretical difficulty since it is worrisome to be faced with perturbation-type results that have acquired such amplitude. Our results therefore indicate that, when calculations are performed within the context of a realistic nuclear potential, the 2p-2h background is indeed small. This further suggests that the higher energy experimental points in the dip region are clearly indicative of *effects beyond the nuclear structure medium* and are consistent with the onset of  $\Delta$ -hole and meson exchange excitations, which have been outside the domain of our preoccupation.

In conclusion, one of the major results of our work has been to demonstrate, we hope conclusively, that theoretical calculations of the nuclear response in the quasielastic peak region and beyond can only achieve agreement with experiment when 2p-2h effects are taken into account. The other major result has been to elucidate the magnitude and structure of the quasielastic peak itself, which is, in our opinion, mainly an RPA effect. It is also comforting to observe that our results are consistent with those of an earlier approach using the Fermi gas model. In the higher energy dip region our calculation still comes below experiment which suggests that extra-nuclear degrees of freedom are at play there.

Recently, Rost, Price, and Shepard [31] have presented an interesting relativistic calculation of the transverse response in the  $\Delta$ -resonance region. These authors obtain good agreement with experiment in a relativistic Hartree approximation in configuration space. In their model the delta is propagated with its free mass and width—pion blocking and pion absorption being taken into account by a single parametrized shift in the position of the delta. The results look promising;

however, most of the improvement seen in the  $^{40}\text{Ca}$  case at  $q=2.78\text{ fm}^{-1}$  is located in the dip region—the strength remaining below the measured value in the region of the quasi-elastic peak. This fact is even more pronounced in  $^{12}\text{C}$  where the calculated results underestimate markedly the peak cross section. We believe this substantiates our claim that the enhancement in the peak is dominated by the nuclear structure whereas extra-nuclear degrees of freedom contribute more markedly to the strength in the dip region.

In the longitudinal context, an interesting development has just unfolded with the recent presentation by Yates *et al.* of experimental data on  $^{40}\text{Ca}$  from Bates [32]. These authors show that, contrary to previous results, their longitudinal response functions show no more than 20% missing strength. It will be of great interest to examine the transverse response and the next few years should thus prove interesting for both theoretical and experimental programs.

The authors are grateful to Hiroshi Sagawa, Yoshiyasu Okuhara, and Satoshi Nozawa for their extensive collaboration and to G. E. Brown for insightful comments. This work was supported in part by the Natural Sciences and Engineering Research Council of Canada.

#### APPENDIX

The purpose of this Appendix is to give precise expressions for the ground state amplitudes in Eq. (4) and for the 2p-2h matrix elements in Eq. (7).

The matrix element for the meson exchange interaction

$$\int_0^\infty r^2 dr R_{n_p l_p}(r) j_l(qr) R_{n_h l_h}(r) = \left[ \frac{(2l_p + 2n_p + 1)!! (2l_h + 2n_h + 1)!!}{2^{n_p + n_h} n_p! n_h!} \right]^{1/2} \sum_{k=0}^{n_p} \sum_{k'=0}^{n_h} (-)^{k+k'} \begin{bmatrix} n_p \\ k \end{bmatrix} \begin{bmatrix} n_h \\ k' \end{bmatrix} \times \frac{(l + l_p + l_h + 2k + 2k' + 1)!!}{(2l_p + 2k + 1)!! (2l_h + k' + 1)!!} e^{q^2/4\nu} \sum_{m=0}^M (-)^m \begin{bmatrix} M \\ m \end{bmatrix} \frac{q^{2m+l}}{(2m + 2l + 1)!! (2\nu)^{m+l/2}}, \quad (\text{A3})$$

where  $M = (l_p + l_h - l)/2 + k + k'$  is an integer. The constant  $\nu$  is defined in terms of the oscillator frequency  $\omega$  (using  $\omega = 41A^{-1/3}$ ) and the nucleon mass  $m_n$  to be

$$\nu \equiv m_n \omega / \hbar, \quad (\text{A4})$$

and, in the usual notation,

$$\begin{bmatrix} n \\ k \end{bmatrix} \equiv \frac{n!}{k!(n-k)!}. \quad (\text{A5})$$

The term  $\hat{W}_J(\omega, q)$  in Eq. (A1) contains the information on the particle-hole interaction and takes the form

$$[\hat{W}_J(\omega, q)]_{LL'} \equiv a_{JL} V_\pi(\omega, q) a_{JL} + b_{JL} V_\rho(\omega, q) b_{JL} + (f_\pi^2/m_\pi^2) \Gamma_\pi^2 g' \delta_{LL'}. \quad (\text{A6})$$

The interaction strengths  $V_\pi$  and  $V_\rho$  are given by

$$V_\pi(\omega, q) = (f_\pi^2/m_\pi^2) \Gamma_\pi^2 q^2 / (\omega^2 - q^2 - m_\pi^2), \quad (\text{A7})$$

that excites virtual 2p-2h states has been determined by Oset, Toki, and Weise [29] to be

$$a_i = \langle (p'h') J' M' T' M'_T (ph) J M T M_T | V | \hat{0} \rangle = \delta_{JJ'} \delta_{MM'} \delta_{TT'} \delta_{M_T M'_T} \sum_{LL'} \int_0^\infty \frac{dq}{(2\pi)^3} F_{p'h'}^{JL'}(q) \times [\hat{W}_J(\omega, q)]_{LL'} F_{ph}^{JL}(q). \quad (\text{A1})$$

The  $F_{ph}$  factors are proportional to radial particle-hole transition densities and are given by

$$F_{ph}^{JL} = i^{L+l_p-l_h} \sqrt{48\pi} \hat{L} \hat{j}_p \hat{j}_h \hat{l}_h \begin{pmatrix} l_p & l_h & L \\ 1/2 & 1/2 & 1 \\ j_p & j_h & J \end{pmatrix} \langle L 0 l_h 0 | l_p 0 \rangle \times \int_0^\infty r^2 dr R_p(r) j_L(qr) R_h(r), \quad (\text{A2})$$

with the  $9j$  factor a result of the usual  $LS-jj$  transformation. One of the great advantages of using a harmonic oscillator basis for the wave functions is that, in that particular basis, the radial overlap integral in Eq. (A2) can be expressed analytically thus eliminating the requirement to perform a numerical integration. This has enormous time saving benefits as well as improving the numerical accuracy. This expression can be found in Ref. [30] and is presented here for completeness:

$$V_\rho(\omega, q) = (f_\rho^2/m_\rho^2) \Gamma_\rho^2 q^2 / (\omega^2 - q^2 - m_\rho^2), \quad (\text{A8})$$

where the values of the cutoff masses, coupling constants, and the Landau parameter  $g'$  were taken from Ref. [29]. The  $a_{JL}$  and  $b_{JL}$  coefficients are a result of the angular momentum recoupling. For p-h states that individually couple to unnatural parity they have the form

$$a_{JL} = \sqrt{J/(2J+1)} \quad \text{for } L=J-1, \\ = -\sqrt{(J+1)/(2J+1)} \quad \text{for } L=J+1, \\ b_{JL} = \sqrt{(J+1)/(2J+1)} \quad \text{for } L=J-1, \\ = \sqrt{J/(2J+1)} \quad \text{for } L=J+1. \quad (\text{A9})$$

For p-h states that couple separately to natural parity (i.e.,  $L=J$ ), we have  $a=0$  and  $b=1$ .

With the transverse operator expanded in terms of its multipoles, the bulk of the calculation consists of computing the matrix elements between the ground state and the possible excited states. In this case the initial state is a 2p-2h state

coupled to spin 0 and the final state is also a 2p-2h state but with arbitrary spin  $J_f$  and projection  $M_f$ .

After a good deal of angular momentum recoupling algebra, we arrive at the expression

$$\begin{aligned}
 \langle (2p2h)_k \lambda \mu \| \hat{\mathbf{O}}^\lambda \| (2p2h)_i 00 \rangle &= \langle \{ (j'_{p_1} j'_{h_1}) J'_1 (j'_{p_2} j'_{h_2}) J'_2 \}_k \lambda \mu \| \hat{\mathbf{O}}^\lambda \| \{ (j_{p_1} j_{h_1}) J_1 (j_{p_2} j_{h_2}) J_2 \}_i 00 \rangle \\
 &= \hat{J}'_1 \delta_{J'_2 J_2} \left\{ (-)^{J_1 + j'_{p_1} + j_{h_1} + \lambda} \begin{pmatrix} j_{p_1} & J_1 & j_{h_1} \\ J'_1 & j'_{p_1} & \lambda \end{pmatrix} \langle j'_{p_1} \| \hat{\mathbf{O}}^\lambda \| j_{p_1} \rangle \delta_{h'_1 h_1} + (-)^{j_{h_1} + J'_1 + j_{p_1} + \lambda} \begin{pmatrix} J_1 & j_{h_1} & j_{p_1} \\ j'_{h_1} & J'_1 & \lambda \end{pmatrix} \langle j'_{h_1} \| \hat{\mathbf{O}}^\lambda \| j_{h_1} \rangle \delta_{p'_1 p_1} \right\} \\
 &\quad + \hat{J}'_2 \delta_{J'_1 J_1} (-)^{J_1 + \lambda + J'_2} \left\{ (-)^{J_1 + j'_{p_2} + j_{h_2} + \lambda} \begin{pmatrix} j_{p_2} & J_1 & j_{h_2} \\ J'_2 & j'_{p_2} & \lambda \end{pmatrix} \langle j'_{p_2} \| \hat{\mathbf{O}}^\lambda \| j_{p_2} \rangle \delta_{h'_2 h_2} \right. \\
 &\quad \left. + (-)^{j_{h_2} + J'_2 + j_{p_2} + \lambda} \begin{pmatrix} J_1 & j_{h_2} & j_{p_2} \\ j'_{h_2} & J'_2 & \lambda \end{pmatrix} \langle j'_{h_2} \| \hat{\mathbf{O}}^\lambda \| j_{h_2} \rangle \delta_{p'_2 p_2} \right\}, \quad (\text{A10})
 \end{aligned}$$

where we have introduced the notation  $\hat{J} \equiv \sqrt{2J+1}$ . The large parentheses indicate 6j symbols. The single particle reduced matrix elements of the operator  $\hat{\mathbf{O}}^\lambda$  are given by

$$\begin{aligned}
 \langle j_2 \| \hat{\mathbf{O}}^\lambda \| j_1 \rangle &= \sum_l i^{l_1 - l_2 + l + 1} q \mu \sqrt{6l^2} \hat{l}_1 \hat{\lambda} \hat{j}_1 \hat{j}_2 \langle l_1 0 l 0 | l_2 0 \rangle \\
 &\quad \times \langle l 0 1 \mu | \lambda \mu \rangle \begin{pmatrix} l_2 & 1/2 & j_2 \\ l_1 & 1/2 & j_1 \\ l & 1 & \lambda \end{pmatrix} \langle j_l(rq) \rangle, \quad (\text{A11})
 \end{aligned}$$

where the symbol  $\langle j_l(rq) \rangle$  is used to represent the radial overlap integral given by

$$\langle j_l(rq) \rangle \equiv \int_0^\infty r^2 dr R_2(r) j_l(qr) R_1(r), \quad (\text{A12})$$

where  $j_l(qr)$  is a spherical Bessel function and the parentheses indicate a 9j symbol.

- [1] E. J. Moniz *et al.*, Phys. Rev. Lett. **26**, 445 (1971).  
 [2] R. Altemus *et al.*, Phys. Rev. Lett. **44**, 965 (1980).  
 [3] T. deForest and J. D. Walecka, Adv. Phys. **15**, 1 (1966).  
 [4] P. Barreau *et al.*, Nucl. Phys. **A402**, 515 (1983); **A358**, 287c (1981).  
 [5] C. C. Blatchley *et al.*, Phys. Rev. C **34**, 1243 (1986).  
 [6] M. Deady *et al.*, Phys. Rev. C **33**, 1897 (1986); **28**, 631 (1983).  
 [7] A. Hotta *et al.*, Phys. Rev. C **30**, 87 (1984).  
 [8] Z. E. Meziani *et al.*, Phys. Rev. Lett. **52**, 2130 (1984); **54**, 1233 (1985); Nucl. Phys. **A46**, 113c (1985).  
 [9] W. Alberico *et al.*, Nucl. Phys. **A462**, 269 (1987).  
 [10] F. A. Bireva and A. Dellafiore, Phys. Rev. C **36**, 899 (1987).  
 [11] P. M. Boucher *et al.*, Phys. Lett. B **219**, 10 (1989); Ann. Phys. (N.Y.) **196**, 150 (1989).  
 [12] M. Cavinato *et al.*, Nucl. Phys. **A423**, 376 (1984).  
 [13] L. S. Celenza *et al.*, Phys. Rev. C **31**, 946 (1985).  
 [14] J. P. Chen *et al.*, Phys. Rev. Lett. **66**, 1283 (1991).  
 [15] G. Co' *et al.*, Nucl. Phys. **A485**, 61 (1988).  
 [16] A. Dellafiore *et al.*, Phys. Rev. C **31**, 1088 (1985).  
 [17] G. Do Dang and N. van Giai, Phys. Rev. C **30**, 731 (1984); see also X. Ji, Phys. Lett. B **219**, 143 (1989).  
 [18] C. Drozd *et al.*, Phys. Lett. B **185**, 287 (1987).  
 [19] H. Kurasawa and T. Suzuki, *Proceedings of the Workshop on Relativistic Nuclear Many-Body Physics* (World Scientific, Teaneck, NJ, 1988).  
 [20] H. Kurasawa and T. Suzuki, Phys. Lett. B **208**, 160 (1988); **211**, 500 (1988).  
 [21] J. V. Noble, Phys. Rev. Lett. **46**, 412 (1981).  
 [22] R. D. Smith and J. Wambach, Phys. Rev. C **38**, 100 (1988).  
 [23] U. Stroth, R. W. Hasse, and P. Schuck, Phys. Lett. B **171**, 339 (1986).  
 [24] W. Alberico *et al.*, in *Proceedings of the Workshop on Electron-Nucleus Scattering*, edited by A. Fabrocini *et al.* (World Scientific, Teaneck, NJ, 1988), p. 430; Phys. Rev. C **34**, 977 (1986).  
 [25] W. M. Alberico, M. Ericson, and A. Molinari, Nucl. Phys. **A379**, 429 (1982).  
 [26] G. F. Bertsch and S. F. Tsai, Phys. Rep. **18**, 125 (1975).  
 [27] S. Shlomo and G. F. Bertsch, Nucl. Phys. **A243**, 507 (1975).  
 [28] J. Speth *et al.*, Nucl. Phys. **A343**, 382 (1980).  
 [29] E. Oset, H. Toki, and W. Weise, Phys. Rep. **83**, 281 (1982).  
 [30] W. M. Alberico, A. DePace, and A. Molinari, Phys. Rev. C **31**, 2007 (1985).  
 [31] E. Rost, C. E. Price, and J. R. Shepard, Phys. Rev. C **47**, 2250 (1993).  
 [32] T. C. Yates *et al.*, Phys. Lett. B **312**, 382 (1993).